Solar Energy 299 (2025) 113716

Contents lists available at ScienceDirect

Solar Energy

journal homepage: www.elsevier.com/locate/solener

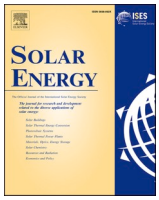

Solar energy for greenhouse drying: Performance evaluation of parabolic trough solar collector with two-axis tracking system

Mehmet Das [a,1,*], Oguzhan Pektezel [b,2], Mithat Sımsek [c,3]

[a] Mechanical Engineering Department, Engineering Faculty, Firat University, 23279 Elazig, Turkey
[b] Mechanical Engineering Department, Balikesir University, 10145 Balikesir, Turkey
[c] Mechanical Engineering Department, Tokat Gaziosmanpasa University, 60250 Tokat, Turkey

ARTICLE INFO

Keywords:
Parabolic trough solar collector
Greenhouse dryer
Heat and mass transfer
Two-axis solar tracking system

ABSTRACT

This study was conducted to develop a solution for the efficient and sustainable use of solar energy in food drying in response to the depletion of fossil fuels, environmental concerns, and increasing energy demand. The motivation is to improve energy efficiency and provide environmentally friendly alternatives in food drying applications. This study experimentally evaluated the performance of a greenhouse dryer equipped with a parabolic trough solar collector (PTSC) with an air-fluidized, dual-axis solar tracking system (STS). The experiments were conducted between June 12 and June 17, 2023, in Tokat, Turkey, located between 39°51′–40°55′ North latitudes and 35°27′–37°39′ East longitudes, between 10:00 a.m. and 5:00p.m. each day. In the apple drying experiments, solar radiation was continuously directed to the collector at an optimum angle with STS, and energy efficiency and exergy efficiency increased by 28.7 % and 36.2 %, respectively. Drying time decreased by 57.2 %, and the product surface temperature reached 76.1 °C. With the effect of STS, solar radiation on the system increased by an average of 18.8 %, and drying efficiency improved by 47.2 %. The study's originality is using air-fluid in the tube system, which is equipped with a dual-axis, fully automatic solar tracking mechanism. In the literature, water-based and single-axis systems have generally been studied. This study introduces an innovation that enhances the efficiency and sustainability of solar energy usage in food drying. It offers a transformative approach to integrating energy systems within agricultural practices, paving the way for a more effective and environmentally friendly future in food drying.

1. Introduction

The serious problems faced in the energy field today are the rapid depletion of fossil fuels, the increasing effects of global warming, and the ever-growing demand for electricity [1] Solar energy is a sustainable alternative that can solve these challenges [2]. The fact that it is an abundant and accessible resource makes it very attractive regarding energy production. The sun sends about 1.7 × 1014 kW of energy to the earth's surface every year, and even a small fraction of this amount is enough to meet global energy needs [3]. Solar energy, which is also advantageous in flexibility and convertibility, can be used in electricity generation and heating applications. In addition, the high energy content of the radiation emitted from the sun enables this resource to offer a wide range of applications [4]. All these features make solar energy a renewable option with environmental and economic benefits.

Technologies developed for the practical use of solar energy include thermal solar collectors and photovoltaic cells. Thermal collectors collect solar radiation and convert it into usable heat, while photovoltaic cells generate electricity directly. Thermal collectors fall into two main categories: flat-plate collectors and concentrator-type systems. While flat-plate collectors can generally generate temperatures of up to 90 °C, evacuated tube collectors raise this limit to 150 °C [5]. For applications requiring higher temperatures, concentrator systems come into play; these systems can operate in the 150–500 °C temperature range [6]. PTSC are considered the most advanced technology among concentrator systems and excel in efficiency and longevity [7]. Developing these technologies and making them more accessible will increase solar

* Corresponding author.
E-mail addresses: m.das@firat.edu.tr (M. Das), oguzhan.pektezel@balikesir.edu.tr (O. Pektezel), mithat.simsek@gop.edu.tr (M. Sımsek).
[1] Orcid:0000-0002-4143-9226.
[2] Orcid:0000-0002-8356-181X.
[3] Orcid:0000-0002-0534-1133.

https://doi.org/10.1016/j.solener.2025.113716
Received 8 February 2025; Received in revised form 30 May 2025; Accepted 19 June 2025
Available online 2 July 2025

Nomenclature

Symbol/Abbreviation

PTSC	Parabolic Trough Solar Collector (—)
STS	Solar Tracking System (—)
GD	Greenhouse Dryer (—)
LDR	Light Dependent Resistor (—)
PLC	Programmable Logic Controller (—)
T_1,T_i	Dryer Inlet Temperature (°C)
T_2,T_o	Dryer Outlet Temperature (°C)
T_3,T_a	Ambient Temperature (°C)
T_4,T_{po}	Tube Outlet Temperature (°C)
T_5, T_6	Product Surface Temperatures (°C)
T_7	Inside Dryer Temperature (°C)
T_{pi}	Tube Inlet Temperature (°C)
H_1, H_2, H_3	Relative Humidity Values (%)
V	Air Velocity (m/s)
W	Product Weight (g)
W_k	Dry Product Weight (g)
W_s	Wet Product Weight (g)
WS	Wind Speed (m/s)
MC_w	Moisture Content (wet basis) (%)
$MC_{d.b}$	Moisture Content (dry basis) (%)
M_e	Equilibrium relative humidity value (g water/g solids)
M_o	Initial Product Weight (g)
MR	Moisture Ratio (Dimensionless)
η_{th}	Thermal Efficiency (%)
η_d	Drying Efficiency (%)
η_{exergy}	Exergy Efficiency (%)
Q_u	Useful Heat Energy (kJ)
Q_s	Heat Energy Absorbed by the PTSC (kJ)
A_a	Collector Aperture Area (m^2)
I_b, SR	Global Solar Radiation (W/m^2)
L_r, W_r	Reflector Dimensions (Length/Width) (m)
L_w	Latent heat of evaporation (540) (kcal/kg)
A_a	Arpeture Area (m^2)
C_g	Geometric Concentration Ratio (—)
ψ	Reflector Rim Angle (°)
C_p	Specific Heat Capacity (kJ/kg·K)
ET	Energy Consumption Of The System Components (kJ)
Q_s	Absorbed Solar Heat by Collector (kJ)
T_{pi}, T_{po}	Collector Inlet and Outlet Temperatures (K)
T_{sun}	Sun Surface Temperature (4350) (K)

energy's role in meeting the world's energy needs. In addition, these systems' high efficiency and diversity are accelerating developments in the renewable energy sector. In the future, such environmentally friendly methods of energy production will contribute to both sustainable development and environmental protection goals.

The literature contains many valuable scientific studies of PTSCs. These studies have examined the energy performance of parabolic solar collectors in power generation, food drying, and various hot fluid processes. Othman et al. used a thermal oil parabolic solar collector for an olive mill sludge drying system in Borj Cedria, Tunisia. They designed a heat exchanger to heat the air with hot oil from the solar collector. They used the hot air from the heat exchanger to dry the olive sludge. With this heat exchanger, they obtained drying air at a temperature of 128 °C at an air velocity of 3 m/s [8]. Nain et al. investigated the thermal performance of a vacuum tube parabolic solar collector in Haryana, India by passing air fluid through the collector. As a result of their study, they obtained an average of 95 °C hot air for an air flow rate of 4.5 kg/h [9]. Mathew et al. used a water parabolic solar collector to store energy in a thermal store. They used this storage as a heat exchanger and obtained hot air for drying apples. They obtained a maximum temperature of 118 °C at an air velocity of 2 m/s [10]. Guan and others designed a new parabolic trough solar air collector (PTSAC-TRT) with triple receiver tubes to address the issues of high outlet temperatures and significant temperature differences between the inlet and outlet in parabolic trough collectors (PTCs). They set the air velocity in the PTC to 5.4 m/s and achieved an instantaneous collection efficiency (ICE) of up to 76.0 % [11]. Limboonruang et al. investigated the increase in thermal efficiency of PTC using seven suction tube models with different finned tube characteristics. In a PTC with finned suction tubes having a fin spacing of 2.28 mm and a fin diameter of 22 mm, they achieved a maximum temperature increase of 9.60 °C and a thermal efficiency of 58.66 % at a flow rate of 1.0 L/min [12]. Parlamış et al. passed air in different geometries in a parabolic corrugated vacuum tube solar collector in Konya, Turkey. With a copper helical helix placed inside the vacuum tube, they obtained an average of 20 % more energy efficiency than the empty vacuum tube [13]. Pandey et al. placed a U-tube copper tube inside the vacuum whole in a parabolic trough vacuum tube solar collector system in Himachal Pradesh, India. Their study obtained 151 °C hot air at a mass flow rate of 0.0062 kg/s [14].

Solar tracking mechanisms have been used for solar energy systems to maximize the benefit of solar radiation. The performance of solar energy systems has increased significantly due to tracking systems. The literature contains many valuable studies on parabolic solar collectors with solar tracking mechanisms. Stanek et al. installed a manually controlled two-axis solar tracking mechanism on Poland's vacuum tube aqueous parabolic solar collector. They investigated both the effects of the solar tracking system on energy performance and solar tracking errors [15]. Gharzi et al. added a thermoelectric system and a two-axis ardinuo-powered solar tracking system to an aqueous parabolic trough solar collector in Gorgan, Iran. They operated the solar tracking system according to the ardinuo command system and investigated the effects of the tracking system on electrical and thermal energy performance [16]. Wang et al. developed a single-axis tracking model using the Solar Position Algorithm (SPA) for PTC and analyzed the operating characteristics of the collector. Through comparative analysis of tracking angles and field tests, they verified the robustness and overall performance of the system in distributed heating applications [17]. Fathabadi designed a two-axis solar tracking mechanism to improve the thermal performance of an aqueous vacuum tube parabolic solar collector and provided axis tracking control with microcontrollers [18]. Saldivar-Aguilera and others have investigated a dual closed-loop control strategy for single-axis solar tracking systems in PTC. They conducted a comparative analysis between the proposed control algorithm and a simple closed-loop control typically used in PTC. The experimental results they obtained indicated that the average solar tracking error achieved with the simple control was 0.97°, while the error of the proposed dual control was 0.21° [19].

Furthermore, a wealth of significant research has been carried out on hybrid systems integrated with solar greenhouse dryer systems, as detailed in Table 1. This table categorizes the studies based on energy sources, system types, and performance enhancements and summarizes the innovative advancements achieved, providing a clear comparison with the current study.

When the studies in the literature on PTSC were analyzed, some of the following study gaps were identified.

1. Low airflow rates have generally been studied. This is because the tube's heat transfer area is insufficient.
2. Since hot air is produced with a single tube, it is insufficient for processes requiring a high hot air flow rate.

Table 1
Comparison of studies related to solar greenhouse dryers with the current study.

Reference	Energy Source	System Type	Performance Improvement	Innovation Summary
Arbaoui et al. [20]	Solar Energy (Conversion of agricultural greenhouse to dryer)	Indirect Greenhouse Dryer (Double-glazed roof + thermal storage)	Copper pipe heat collector on roof and forced hot air flow	Seasonal conversion of greenhouse into dryer for dual usage (farming + drying)
Tiguh et al. [21]	Solar Energy (Dual-shaped design)	Dual-Shaped Greenhouse Dryer	Higher load/volume ratio and improved land use efficiency	New dual-shaped design for improved drying quality and economic performance
Zine et al. [22]	Solar Energy (Natural and forced convection greenhouse dryer)	Natural and Forced Convection Greenhouse Dryer	Adaptation to climatic conditions with optional forced fan mode	Customized greenhouse dryer solution for Teff farming
Rajesh et al. [23]	Solar Energy (New generation greenhouse dryer – NGHD)	New Type Greenhouse Dryer (Sandwich-panel insulated structure)	Thermally insulated drying chamber and black painted absorber surfaces	32 % faster drying compared to conventional greenhouse dryers with better product quality
Patel et al. [24]	Solar Energy (Greenhouse dryer with glass material variations)	Passive and Active Greenhouse Dryer (DL and UVP coated glasses)	Comparison of double-layer and UV-protected glass coatings	Performance improvement with DL-coated glass in greenhouse dryer
Sehrawat et al. [25]	Solar Energy (Portable greenhouse solar dryer with ETAH)	Portable Active Greenhouse Dryer (Fan + ETAH + air distribution system)	Circulating fans, evacuated tube solar air heater, air management system	Thermal efficiency enhancement up to 60 % by optimized air flow management
Philip et al. [26]	Solar Energy (Parabolic hybrid greenhouse dryer)	Parabolic Hybrid Active Greenhouse Dryer (SAH assisted)	Integration of solar air heater for drying acceleration	Drying time reduced by up to 30 % using parabolic hybrid design
Koli et al. [27]	Solar Energy (100 kg capacity greenhouse solar dryer)	Large Capacity Greenhouse Solar Dryer	Increase in drying area and product capacity with economic evaluation	Short drying time with low operational cost for high-volume agricultural products
Selimefendigil et al. [28]	Solar Energy (Parabolic hybrid active greenhouse solar dryer)	Parabolic Hybrid Active Greenhouse Solar Dryer (PHAGSD)	Solar air heater integration to enhance drying efficiency and reduce drying time	30 % reduction in drying time and improved drying uniformity with parabolic hybrid system
Singh et al. [29]	Solar Energy (Greenhouse dryer with latent heat thermal storage using nano-paraffin)	Active Greenhouse Dryer + Al_2O_3 Nano-paraffin Thermal Storage System	Latent heat thermal storage unit integration using nano-enhanced paraffin	15 % enhancement in thermal efficiency and specific moisture removal rate improvement
Singh et al. [30]	Solar Energy (Greenhouse dryer with evacuated tube solar air heater)	Greenhouse Dryer + Evacuated Tube Solar Air Heater (Walk-in type)	Air heating via evacuated tube solar collector; insulated north wall; semi-continuous and batch mode tested	Energy and cost payback periods of 2.95 and 1.10 years; CO2 mitigation of 209.21 tons over 20 years
Singh et al. [31]	Solar Energy (Hybrid active greenhouse dryer with ETC)	Hybrid Active Greenhouse Solar Dryer (HAGSD) with internal heat exchanger	Evacuated tube collector heat exchanger bed; forced air circulation	Drying time reduction up to 61.9 %; significant CO2 mitigation compared to conventional dryers
Karthikeyan et al. [32]	Solar Energy (Hybrid active greenhouse dryer with ETC)	Hybrid Active Greenhouse Solar Dryer (HAGSD)	Higher convective and evaporative heat transfer coefficients with ETC integration	New drying kinetic model developed for better prediction of moisture ratio
Current Study	Solar (Parabolic Tube + Dual-Axis Tracking)	PTSC + Dual-Axis Solar Tracking System	Drying time reduced by 57.2 %, efficiency improved by 80 %	The first use of a fully automatic dual-axis tracking system with air-based PTSC

3. Using solar tracking systems to utilize the sun in PTSC systems effectively is rare.
4. Tracking mechanisms are not fully automatic PLC (Programmable Logic Controller) systems with LDR (Light Dependent Resistor) sensors. It is usually manual and single-axis.
5. Water is generally used as a fluid in PTSCs. Food drying studies using air fluid are very rare.

This study investigated the performance of a greenhouse dryer operating air-fluid with a two-axis sun-tracking mechanism to fill the above-mentioned literature gaps. High air temperatures were obtained with the sun-tracking feature of the parabolic tube collector, and adequate drying conditions were obtained. Drying with and without solar tracking and drying in open sun conditions were compared. The parabolic trough collector technology, which usually works with liquid fluid, was tested with air-fluid in this study and obtained high drying performance. This study is one of the rare studies in the field.

2. Material and methods

2.1. Experimental procedure

In the greenhouse dryer (GD) with PTSC, 15 mm thick oval cut and hollowed apple slices were used in the climatic conditions of Tokat province. Drying operations were carried out on 12–17 June 2023. A total of 6 drying experiments were carried out with and without STS. The climatic conditions (temperature, humidity, wind speed, and solar radiation) were similar on the dates of the experiments. In the study, experiments were carried out for 3 days (12–14 June) in the PTSC greenhouse dryer with STS, and the results were averaged. The same procedure is valid for PTSC without STS (15–17 June). The schematic representation of the equipment and measurement parameters of the greenhouse drying system with PTSC is given in Fig. 1.

Table 2 lists the measurement sensors used in the experiments and their specifications. It also details sensor sensitivities, measurement ranges, and brands. Table 3 shows the geometrical properties of the reflector and receiver in the PTSC system. Oval-cut apple slices of 15 mm thickness and 150 g were placed on the drying trays, and the experiments were stopped when the weight changes during the drying process were less than 0.5 g. One commonly used method to determine that the drying process is complete is to wait for the weight change over a specific period to be very small—typically ± 0.5 g or less [33]. This method indicates that the product is no longer losing moisture and has reached its equilibrium moisture content [34]. A small change threshold of 0.5 g is highly sensitive and reliable, especially when using load-cell sensors. This criterion aims to standardize the experiment, ensure comparability between different experiments, and prevent over-drying of the product.

The PLC controlled the drying speed. In the experiments, fan speed control can be used in the PLC system to control the drying airspeed. The drying airspeed is 1.5 m/s in all experiments. The parameters and units measured during the experiments are given in Table 4. The PLC system recorded the data obtained from the experiments in the data logger at one record per second. In this way, changes in the data could be observed immediately.

The geometric concentration ratio of the PTSC system is one of the basic performance criteria and is calculated using Eq. (1). Eq. (1) is

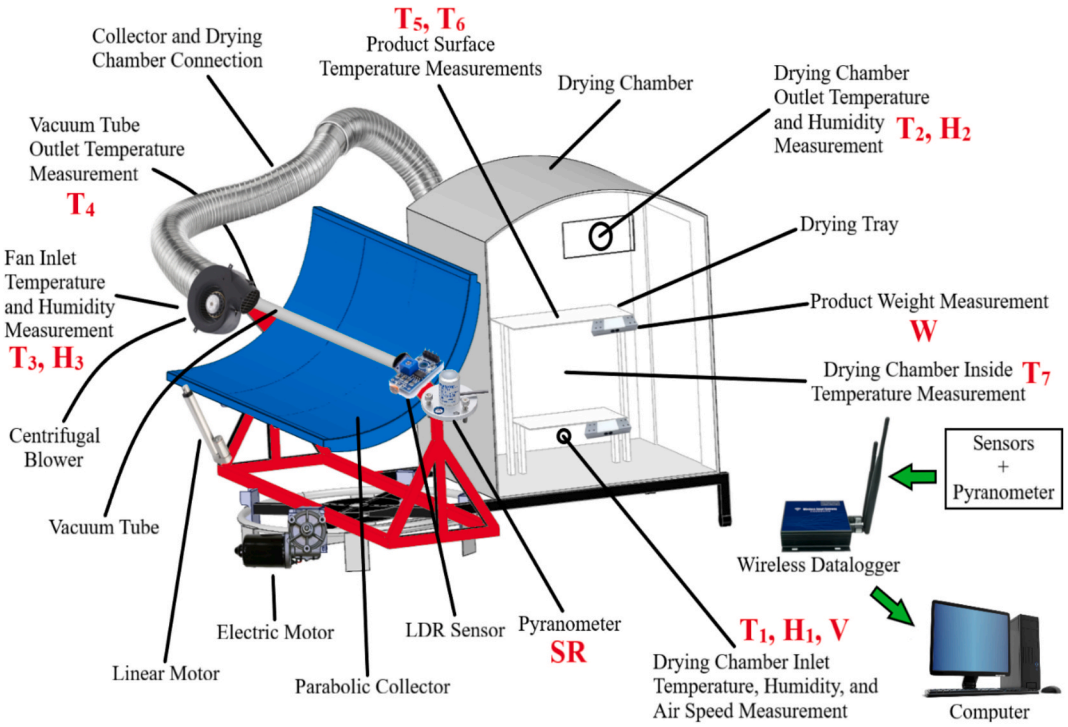

Fig. 1. System elements and measurements.

Table 2
Sensor specifications.

Sensor	Measuring Range	Brand	Accuracy
Air Velocity Transmitter	0 to 20 m/s	HK Instruments	±0.2 m/s
Light Dependent Resistor	20 kΩ to 100 kΩ	RS Components	±0.5 kΩ
PT100	−50 °C to 205 °C	Baumer	±0.3 °C
Pyranometer	0 to 2000 W/m^2	Kipp & Zonen	±0.2 W/m^2
Load cell	10 kg	Zemic	Output Sensitivity ± 0.5 mV/V
Temperature & Relative Humidity	−40 °C to 125 °C & 0 to 100 %	DFROBOT	±0.3 °C & ±3%

Table 3
Geometrical properties of the reflector and receiver.

Parameter	Unit	Value
Length (reflector/receiver)	L_r	2 *m*
Diameter (receiver)	D	0.057 *m*
Width (reflector)	W_r	1.2 *m*
Focal distance (reflector)	*f*	0.27 *m*
Receiver area (receiver)	A_r	0.32 m^2
The rim angle (reflector)	ψ	83.6°
Geometric concentration ratio (receiver)	C_g	6.7
Aperture area (reflector)	A_a	3.6 m^2

defined as follows: A_a; reflector aperture area (collected radiation area); A_r; receiver surface area (heat-transferring surface); W_r; reflector aperture; D; receiver tube diameter; and L_r; receiver length [35]. Fig. 2 schematically presents the geometric parameters of the PTSC.

$$C_g = \frac{A_a}{A_r} = \frac{W_r x L_r}{\pi \text{ xD} x L_r} = \frac{W_r}{\pi \text{ xD}} \quad (1)$$

Fig. 3A shows the airflow and heating process inside the tube. Fresh air drawn from the outside environment by a fan is heated by solar energy as it travels through a 50 mm diameter copper pipe in the center of the tube. The heated air is directed to the greenhouse drying chamber at the end of the tube. Here, it comes into contact with the products, facilitating moisture removal. The figure demonstrates that the airflow path is controlled and that all components work in an integrated manner to ensure efficient heat transfer.

Table 4
Parameters measured in the experiments.

Parameter	Unit	Symbol
Greenhouse Dryer Inlet Temperature	°C	*T1*
Greenhouse Dryer Outlet Temperature	°C	*T2*
Ambient Temperature (Tube Inlet Temperature)	°C	*T3*
Tube Outlet Temperature	°C	*T4*
Product Surface Temperature-1	°C	*T5*
Product Surface Temperature-2	°C	*T6*
Greenhouse Dryer Inside Temperature	°C	*T7*
Solar Radiation	W/m^2	*SR*
Greenhouse Dryer Inlet Relative Humidity	%	*H1*
Greenhouse Dryer Outlet Relative Humidity	%	*H2*
Ambient Relative Humidity	%	*H3*
Greenhouse Dryer Inside Relative Humidity	%	*H1*
Ambient Relative Humidity	%	*H2*
Air velocity	m/s	*V*
Electric Consumption	Wh	*Watt*
Product Weight	gram	*W*

The hot air obtained at the PTSC outlet is maintained at a temperature of 60–80 °C by the system controllers and fan-assisted air circulation, considering the product's drying curve. This range corresponds to the optimum drying temperature recommended for many agricultural products [36,37]. Hot air is drawn in from the PTSC outlet, as shown in Fig. 3B and directed directly to the drying tray via a fan. The airflow is distributed so that it affects the lower surface of the product. Since there is only a single tray in the system, the airflow passages are simple. This situation has positively affected temperature control and energy management.

The components of the GD system with PTSC and the elements of the 2-axis STS are shown in Table 5. Fig. 4 shows the dual-axis STS elements of the PTSC.

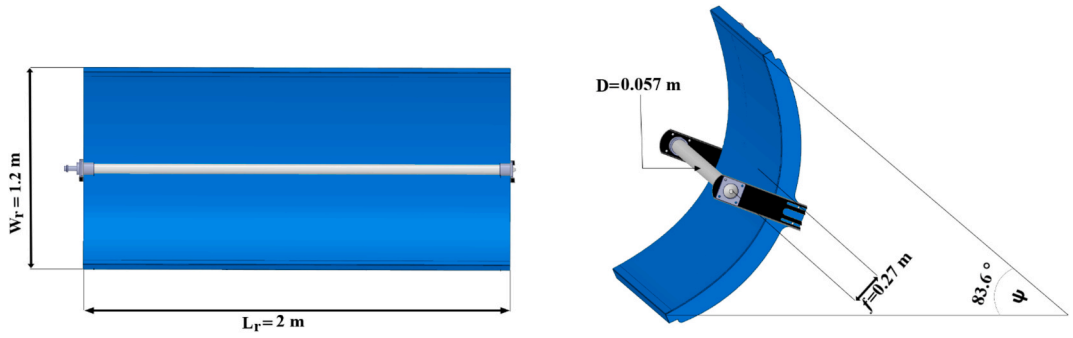

Fig. 2. Dimensions of PTSC.

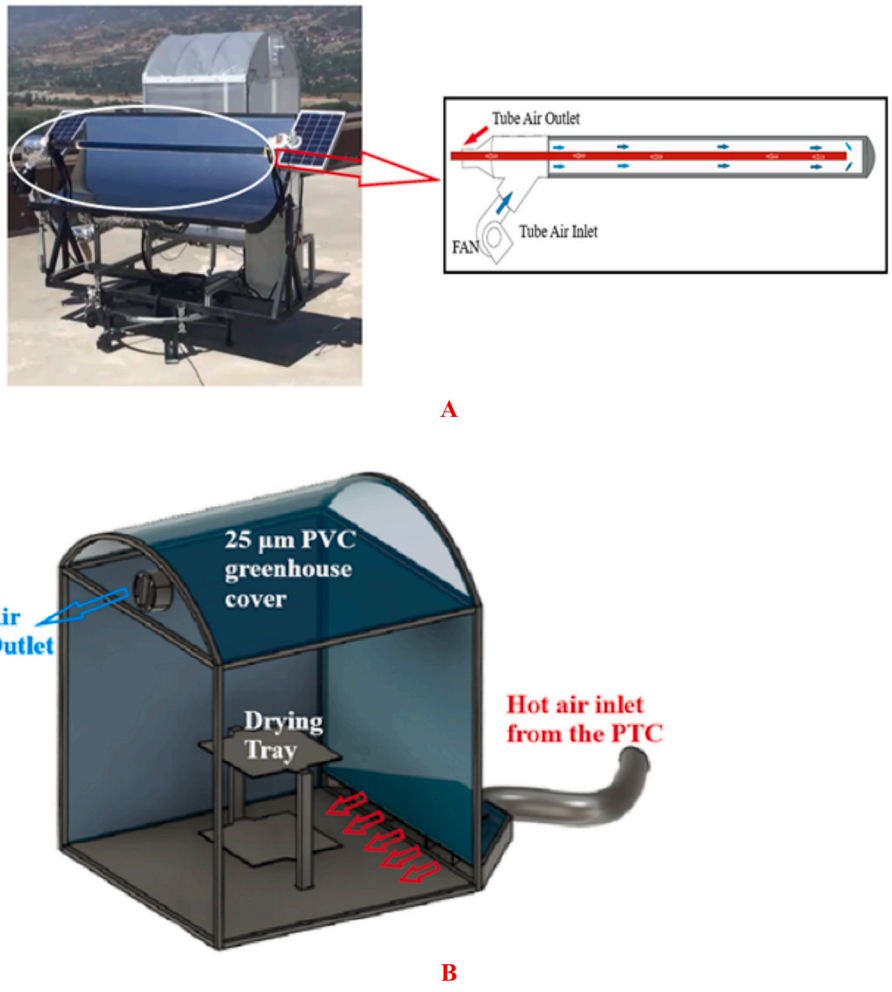

Fig. 3. Airflow and Heat Transfer Process Inside the Tube (A), Air distribution in the drying chamber (B).

The STS system in the PTSC_GD system operates in on/off control mode. When STS is activated, the LDR sensor tracks the sun so that it is perpendicular to the sensor at 90 degrees. For this purpose, it uses the motor and operating system shown in Fig. 4. When STS was deactivated, the PTSC system is fixed in a southeast direction with a tilt angle of 37.2 degrees for Tokat province. For this arrangement, angle control and manual control modes are used. Thus, the same system operates both with STS and without STS.

Fig. 4A shows the mechanical and electronic components of a dual-axis solar tracking system designed to position a parabolic trough solar collector relative to the sun. A high-torque worm gear DC motor provides east–west movement, while a linear DC actuator motor achieves north–south linear movement. The PLC system evaluates light intensity data from LDR sensors to ensure that the collector surface remains perpendicular to the sun's rays. This structure is optimized to maximize solar radiation collection and enhance the system's energy efficiency. Fig. 4B shows the PLC operation diagram. The PLC control system processes the irradiance data from the LDR sensors and positions the platform so that the sun's rays fall at a 90° angle to achieve maximum energy harvesting efficiency from sunlight. The system's data logger instantly records parameters such as solar radiation, temperature, and humidity, facilitating analysis of experimental data and optimizing system performance. In addition, the fan transfers hot air passing through the tube to the greenhouse dryer, speeding up the product

Table 5
Properties of PTSC GD system elements.

PTSC GD System Components	Properties	Dimension
Case (PTSC)	1 mm aluminum sigma profile	1100x1200x1500 mm
Case (GD)	0.5 mm aluminum sigma profile	1000x1000x1200
GD cover	Polyethylene, 0.14 mm thickness, 0.65 solar Transmissivity	1000x1000x1200
Fan	Current 0.9 (A), Pressure 350 (Pa), Flow rate 600 (m^3/hour), Speed 1750 (RPM), Power 200 (Watt)	–
Solar Tracking System	Linear DC actuator motor (12–24 V DC voltage, 70 mm stroke, 25 W nominal power), Worm Gear DC reducer (6–24 V DC voltage, 1–200 rpm speed, 30 kg. cm maximum torque)	–
Datalogger	1000 m wireless data transmission, 10 Mbps data transfer rate, 1 TB memory capacity	90x94 mm air outlet duct
PLC	DELTA DVP-ES3 Series, four high-speed counter inputs	7″ display screen

drying process and increasing efficiency.

A total of 6 days of experiments were conducted between June 12 and 17. The climatic conditions on the days of the experiments were quite similar to each other. The average values of the climatic parameters for June 12–14 and June 15–17 are given in Table 6. According to Table 6, the average values for the experiment days for both systems are very close. All experimental days were sunny, and the differences in the average values of the climatic parameters were 6 W/m^2, 0.8 °C, 0.12 m/s, and 2 % for solar radiation (G), ambient temperature (Ta), wind speed (WS), and relative humidity (H), respectively.

2.2. Calculation procedure

The moisture content of food products is evaluated as the amount of water contained in them. Percentage parameters are used to express this amount of water in food. Wet and dry basis definitions are used to determine moisture content. Eq. (2) and Eq. (3) are used to calculate the wet basis (wb) and dry basis (db) moisture contents of the food product [38].

$$MC_{w.b} = \frac{W_s}{W_s + W_k} 100 \tag{2}$$

$$MC_{d.b} = \frac{W_s}{W_k} \tag{3}$$

In Equations, Ws is wet weight, and Wk is dry weight. Dimensionless moisture content (MR) values were calculated using Eq. (4) [39].

$$MR = \frac{M - M_e}{M_o - M_e} \tag{4}$$

In Eq. (4), M_e is the equilibrium relative humidity value of the dried product. The equilibrium moisture content of the apple slices to be dried was determined as 22.9 g water/g solids by Shimadzu MOC63u moisture analyzer.

Thermal efficiency (η_{th}) is the ratio of the useful output Q_u [W] provided by the collector to the global radiation I_b [W/m2] incident on the collector aperture area A_a [m2], the following Eq. (5) expression is used to calculate the thermal efficiency of the air heater [40,41]. Eq. (6) is used here for the aperture area. In this equation, L_r is the length of the collector mirrors, and W_r is the total width of the rectangular aperture.

$$\eta_{th} = \frac{Q_u}{A_a{}^* I_b} = \frac{\dot{m}.C_p.\Delta T}{A_a{}^* I_b} \tag{5}$$

$$A_a = L_r W_r \tag{6}$$

Dryer efficiency is an indispensable factor in measuring the performance of a solar dryer during the drying of food materials and can be quantified as shown in Eq. (7) [42]. In the calculations of drying efficiency, the total energy quantities used for the amount of material evaporated from the product by the system were evaluated. In this case, for the total energy quantity, the energy consumption of the system components (E_T), the heat energy (Q_s) from the PTSC, and the solar energy (Q_c) directly received from the greenhouse cover per unit time were taken into account. Eq. (7), Qc represents the direct solar energy received through the permeability of the greenhouse cover. This value is calculated by multiplying the greenhouse cover area and the solar radiation value incident on the cover per unit time.

$$\eta_{\ dryer} = \frac{(m_i - m_f)x(L_w + C_{pw}(T_o - T_o)}{E_T + Q_s + Q_c} \quad x100\% \tag{7}$$

Table 6
Average values of the climatic conditions in which the experiments were carried out.

With STS (12–14 June 2024)				Without SAC (15–17 June 2024)			
Ta (°C)	G (Watt/m^2)	WS (m/s)	H (%)	Ta (°C)	G (Watt/m^2)	WS (m/s)	H (%)
29.2	652.14	1.54	29.14	28.4	658.21	1.42	31.06

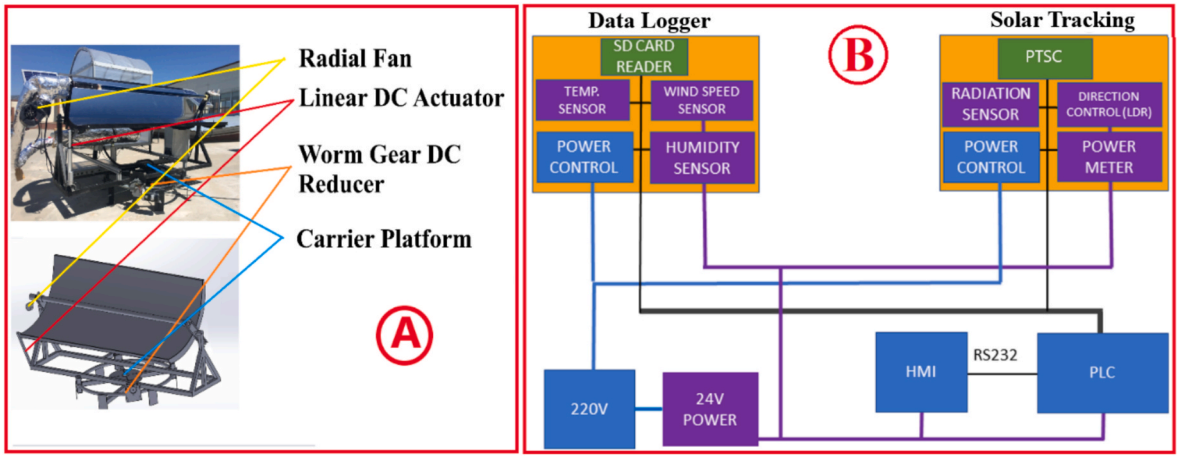

Fig. 4. Mechanical and Electronic Components of the Dual-Axis Solar Tracking System(A) and PLC operation diagram (B).

The PTSC's exergy efficiency is obtained using Eq. (8) based on the solar temperature (4350 K) and the inlet and outlet operating temperatures [43,44]. T_{pi} and T_{po} are the PTSC's inlet and outlet temperatures.

$$\eta_{\text{exergy}} = \frac{\dot{m}C_p\left[\left(T_{po}\text{-}T_{pi}\right)\text{-}T_a\left(\frac{lnT_a}{T_{pi}}\right)\right]}{A_P I_b\left[1\text{-}\left(\frac{T_a}{T_{sun}}\right)\right]} \tag{8}$$

Economic Feasibility Analysis

This section evaluates the economic feasibility of a greenhouse drying unit equipped with a parabolic tube collector and a dual-axis solar tracking system. The analysis was conducted using technical and economic inputs obtained from the user. The data in Table 7 were used for the economic analysis.

Payback Period-PP.

The payback period is a simple financial analysis method that shows how long it will take to recover the cost of an investment [45]. This method is calculated using Eq. (9).

$$\text{Payback period} = \frac{\text{Total system cost}}{\text{Annual net income}} \tag{9}$$

Net Present Value- NPV

NPV is the present value of all a system's profits over its lifetime. Annual profits and costs over the system's lifetime are taken into account. Eq. (10) is used to calculate NPV. A positive NPV indicates the investment is profitable, while a negative NPV may result in a loss [46].

$$\text{NPV} = \sum_{t=1}^{n} \frac{(R_t - C_t)}{(1-r)^t} - I \tag{10}$$

In Eq. (10), − Rt: Net income earned each year, Ct: Maintenance cost in year t, r: Discount rate, n: Economic life of the system, I: Initial investment cost.

3. Results and Dıscussıon

Drying experiments were carried out with and without STS in the GD system with PTSC, and the effects of STS are shown in the results of the following study. Fig. 5 shows the weight changes and *SR* values of the products. The effect of STS was clearly seen in the measured *SR* value and product weight change. With STS, the weight change of the product was very fast, and the wet mass was quickly removed from the product. Drying with STS was 2.27 times faster than drying without STS. A significant increase in *SR* on PTSC was achieved with STS. The average *SR* value increased by 18.8 % using STS. The performance of the GD system with PTSC is illustrated with the temperature variations shown in Fig. 6. There is a significant difference between the temperatures measured in the experiments with and without STS resulting from the increase in *SR* achieved by STS.

Fig. 6. shows that the average GD inlet temperature (*T1*) increased from 47.7 °C to 80 °C with STS. The tube temperature (*T4*) increased on average by 39.8 % with STS. The average product surface temperature (*T5*) was 76.1 °C with STS and 47.3 °C without STS. Fig. 6 shows this increase in temperature profiles with STS, illustrating how the system maximizes solar efficiency and improves drying performance. Furthermore, this difference in temperature values highlights that the STS improves the energy harvesting capacity and the ability to convert this energy to optimize the drying process effectively.

Fig. 7 shows the change in wet and dry base moisture content. In Fig. 7, the amount of liquid substance in the product is removed more quickly if STS is used. Fig. 8 shows the changes in moisture content (MR) with and without STS. The situation is similar to Fig. 7. While the moisture content was stabilized in 185 min with STS, it was stabilized in 420 min without STS.

Fig. 9 shows the energy consumption values for the drying systems with and without STS. When the motor powers providing two-axis solar tracking are included in the STS drying system, the consumption value was measured at an average of approximately 90 Wh. In the without STS drying system, energy consumption is lower and was measured at an average of 30 Wh. Since energy consumption values are included in the drying efficiency values, a decrease in the drying efficiency value of the STS system was observed. When the drying efficiencies are examined overall, the drying efficiency value of the with STS system is approximately two times higher than that of the without STS system.

Fig. 10 compares the drying efficiency over time in greenhouse drying systems with PTSC with and without STS. The figure shows that the system with STS has a clear advantage in drying efficiency; the drying efficiency in the system with STS was measured to be 80 % higher than in the system without STS. This difference can be explained by the fact that the STS captures solar radiation more effectively and increases the inlet temperature of the greenhouse dryer. This higher temperature allows faster removal of moisture from the product. The curve of increase in drying efficiency of the system with STS shows a faster increase with time, indicating that drying time is optimized together with energy efficiency. Fig. 10 highlights this mechanism for improving drying performance and how the solar tracking system plays a critical role in food drying processes in terms of efficiency and sustainability. This important finding clearly illustrates the practical benefits of integrating STS into food drying systems.

Fig. 11 compares the variation of energy and exergy efficiencies over time for greenhouse drying systems with PTSC with and without STS. The figure clearly shows the superior performance of the STS system. In the system with STS, the average energy efficiency increased from 23.2 % to 31.8 %, and the exergy efficiency increased by 60 %. These increases can be explained by the increase in solar radiation intensity (*SR*) shown in Fig. 5 and the increase in temperature profiles shown in detail in Fig. 6. The continuous collection of solar radiation by the STS at the optimum angle increased both the energy gain and the thermodynamic efficiency of the PTSC.

Furthermore, the increase in drying efficiency in Fig. 10 confirms that these energy and exergy gains provided by the STS directly contribute to the drying speed and quality of the products, not just to the system performance. Fig. 11 shows that the increase in exergy efficiency and energy efficiency improves the energy harvesting capacity and the efficiency of the system in utilizing the harvested energy. These results show that the STS is a critical component for food drying processes and energy conversion and sustainability goals. Fig. 11 is a concrete indicator of the technical success of the system and its ability to maximize the use of solar energy.

Let us analyze the drying efficiency results shown in Fig. 10 against similar studies in the literature. The study evaluated the performance of a parabolic trough solar collector greenhouse dryer equipped with a biaxial STS. A significant increase in drying efficiency was observed using the STS. Evaluating these results against similar studies in the literature, Stanek et al. designed an aqueous parabolic collector system using a vacuum tube with a manually controlled biaxial solar tracking system. They observed a significant increase in energy output [15]. However, this study did not use air-fluid; it preferred water. Considering that the system with STS in Fig. 10 is more efficient, the use of air-fluid is

Table 7
Economic analysis inputs.

Parameter	Value
System Cost	1700 USD
Daily Drying Capacity	5 kg/day
Annual Operating Days	300 days/year
Product Sales Price	15 USD/kg
Energy Savings (kWh/day)	1.2 kWh
Electricity Unit Price (USD/kWh)	0.15 USD/kWh
Annual Maintenance Cost	100 USD/year
System Lifespan	15 years
Inflation Rate	35 %

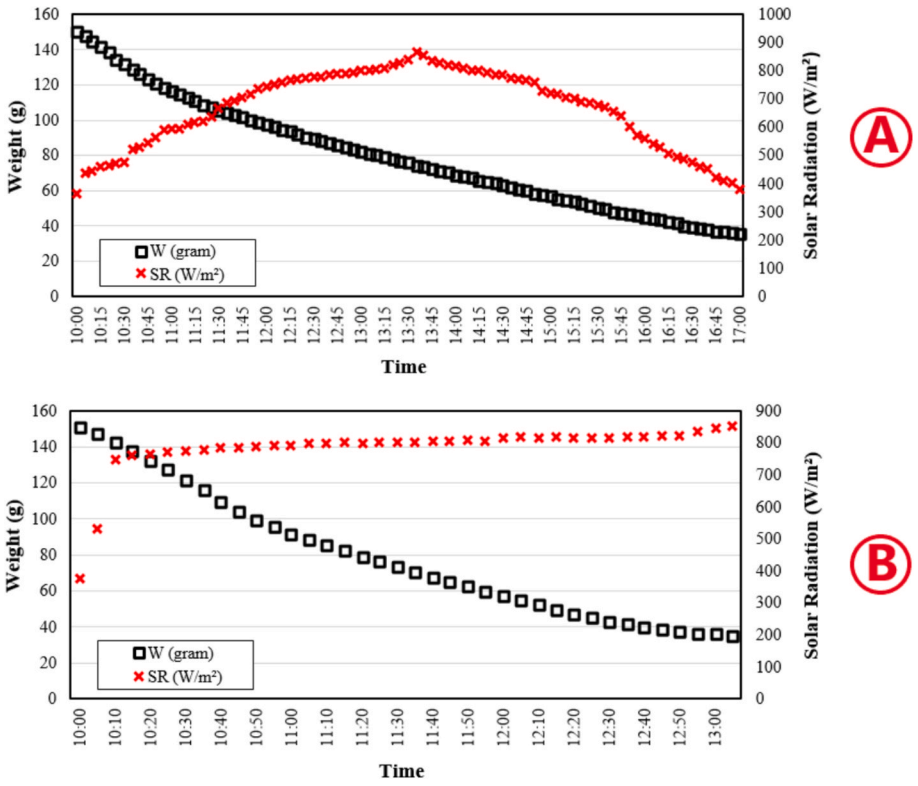

Fig. 5. Variation of *SR* and product weight change (**W**) values with time in the drying system without STS (A) and with STS (B).

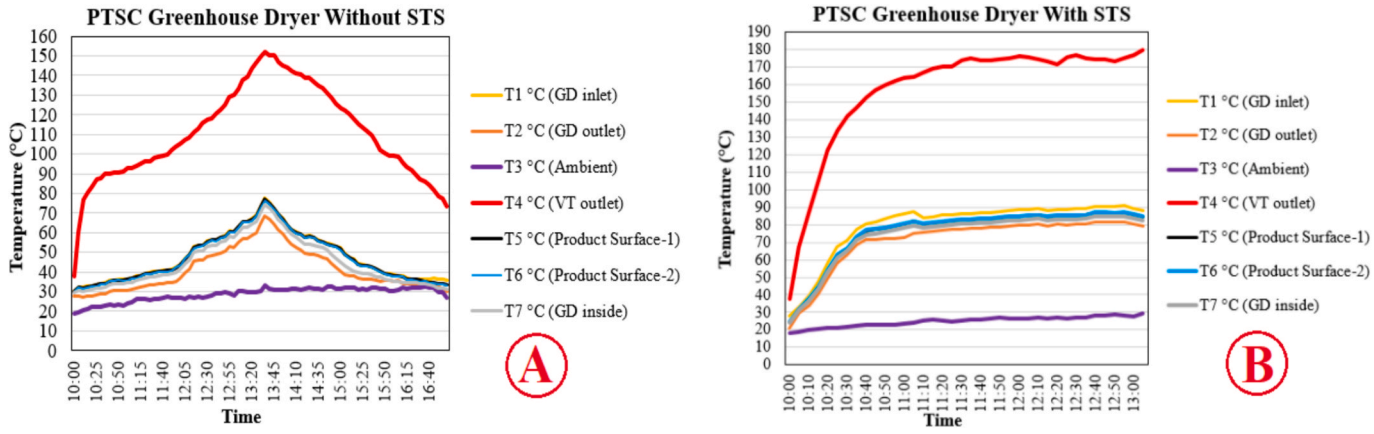

Fig. 6. Variation of temperature values in the drying system without STS (A) and with STS (B) over time.

effective in this increase. Nain et al. reported an increase in thermal efficiency of around 40 % using air-fluid in a vacuum tube parabolic collector [9]. However, as they used a single-axis solar tracking system, the efficiency increase was not as high as in the present study. The advantage of the biaxial system stands out. Fathabadi achieved a 50 % increase in average energy efficiency with a two-axis tracking system [47]. However, the focus was on energy storage rather than drying applications. The effectiveness of two-axis systems in drying processes is more clearly demonstrated in the current study. Büker et al. reported that using copper helical coils in parabolically corrugated vacuum tubes increased energy by 20 % [48]. However, the results in Fig. 10 emphasize that the effect of the tracking mechanism on drying is higher. The results in Fig. 10 show that solar tracking mechanisms significantly increase the energy and drying efficiency of drying processes, particularly in dual-axis applications. Studies in the literature have generally focused on single-axis or manual systems, so the increase from the current study with the STS system is quite remarkable.

The energy and exergy efficiencies presented in Fig. 11 show a high performance compared to the literature's PTSC drying studies. In the present study, an increase in both energy and exergy efficiency was achieved by using the biaxial solar tracking system. Comparison with other PTSC studies in the literature is as follows: Tsongidis et al. optimized thermal energy use with PTSC and achieved around 20 % energy efficiency in drying applications with a responsive energy storage system [49]. Naaim et al. investigated the effect of energy and environmental factors with an air-heated PTSC system and increased energy efficiency by about 25 % [50]. In their study investigating the use of PTSCs with different heat transfer fluids, Houdji et al. reported an energy efficiency of 17.6 % and an exergy efficiency of 9.3 % in drying applications. These values support the superior performance of biaxial tracking systems[51]. Bori et al. optimized the ginger drying process using a PTSC-assisted concentrate-type drying system and reported

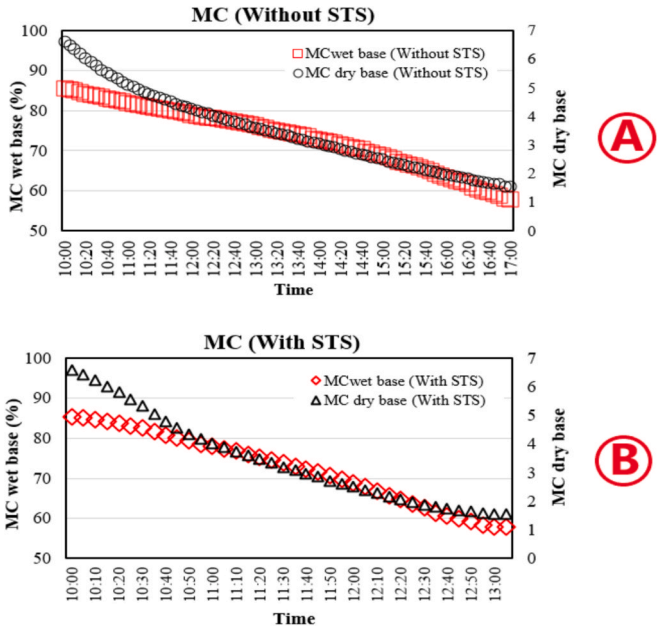

Fig. 7. Variation of moisture content values over time in the drying system without STS (A) and with STS (B).

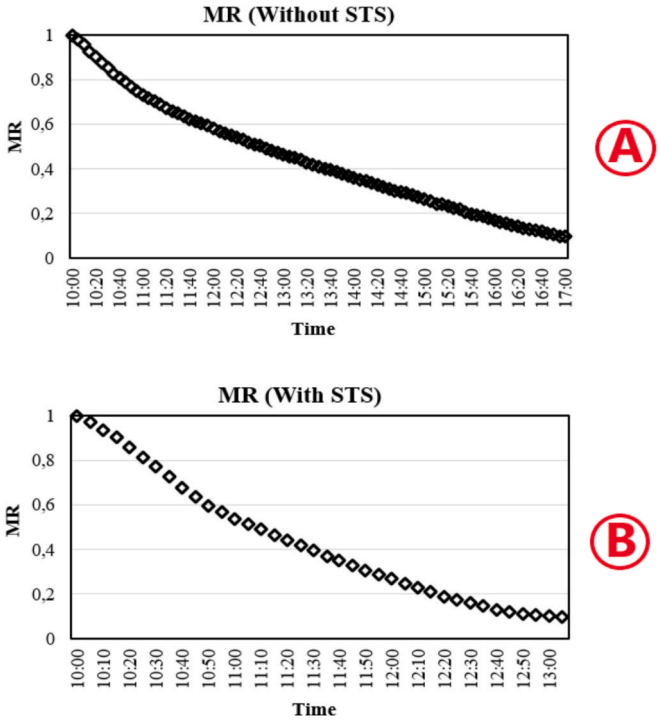

Fig. 8. Variation of the MR values of the drying system without STS (A) and with STS (B) over time.

energy and exergy efficiencies of 22 % and 12 %, respectively [52]. The present study extends this literature by achieving higher results with the biaxial system. Liu et al. (2024) investigated the thermodynamic properties of PTSC for direct steam generation and observed limited increases in energy efficiency [53]. The present study improves energy conversion efficiency by optimizing the drying processes. Other PTSC-based drying studies in the literature generally use fixed or single-axis tracking systems and provide limited improvements in energy efficiency. The results presented in Fig. 11 show that biaxial solar tracking systems provide superior energy and exergy efficiency by continuously capturing solar radiation at the optimum angle. This situation suggests that dual-axis systems may find wider use in PTSC-based applications and that this technology may be more effective in industrial drying processes.

Experimental findings demonstrate that the PTSC-equipped drying system with a dual-axis STS operates significantly more efficiently than its STS-free version. Energy efficiency in the STS-equipped system was bigger than the STS-free system. Similarly, exergy efficiency reached 9.2 % in the STS-equipped system, whereas it remained at 5.7 % in the STS-free system. The tube outlet temperature has increased to 80 °C using STS, which means higher thermal performance than the 57.2 °C in the STS-free system. Drying efficiency has also nearly doubled in the STS-equipped system, reaching 9.5 %, compared to 5 % in the STS-free system. Additionally, the average solar radiation value on the system with the STS represented an 18.8 % increase compared to the system without STS. These data demonstrate that the solar tracking system significantly contributes to energy conversion and drying quality. Table 8 is provided to compare both systems' performance and express the results more clearly.

Economic analysis results.

As a result of the calculated economic parameters for PTSC_GD with STS feature, the system's payback period (PP) was calculated as 0.76 years and the NPV value as 37,421 USD. When the economic analysis of the system is examined, it is seen that it amortizes itself in a short period of approximately 9 months and is highly profitable economically due to the positive NPV value. When examining the economic analysis results of similar systems, Singh et al. [29] found the payback period for a greenhouse dryer supported by SAH to be 1.10 years, while Rajesh et al. [23] found the payback period for greenhouse dryers with different glazing materials to be 0.3–0.5 years, and Singh and Gaur [30] found the payback period for a greenhouse dryer with evacuated tube solar collectors (ETC) to be between 0.69–2.87 years. The payback period in this study is consistent with those in similar studies.

Similar studies in the literature support the results of this study. The PTSC-supported, solar-tracking hybrid greenhouse drying system developed in this study was evaluated regarding key performance indicators such as energy-exergy efficiency, product surface temperature, and economic factors. It achieved more efficient results compared to similar systems in the existing literature. Accordingly, when compared across five different areas:

As examined in terms of STS, the STS system in this study is a PLC-based system with dual-axis movement capability and is capable of instantaneous sun tracking with the aid of an LDR sensor. When examining studies on STS systems developed for PTSC, it was observed that astronomical calculations regarding the sun's position were not used for real-time sun tracking [18,54] and that the STS system did not operate fully automatically for both axes [55,56].

The system's **energy efficiency** showed better performance than the 20 % energy efficiency increase reported in the PTSC-supported dryer in the study by Patel et al. [24].

Exergy efficiency at 9.18 % is significantly higher than the values of 3.01–3.45 % obtained in the Al_2O_3 nanoparticle-based latent heat storage active greenhouse system studied by Selimefendigil et al. [28]. This situation demonstrates the system's superiority not only in terms of heat transfer but also in terms of quality preservation from a thermodynamic perspective.

In terms of **surface temperature**, the STS system reached 77.4 °C, exceeding the temperatures of 53–65 °C obtained in PCM or PVT-supported greenhouse drying systems such as those reported by Arbaoui et al.[20] and Sehrawat et al. [25]. This high temperature accelerates the drying kinetics, increasing drying efficiency to an average of 5.64 %.

From an **economic evaluation** perspective, although the current study does not provide a comprehensive cost analysis, studies by Philip et al. [26] and Mukesh Kumar et al. [57] report that similar systems achieve an investment payback period within 1–2 years. This study's

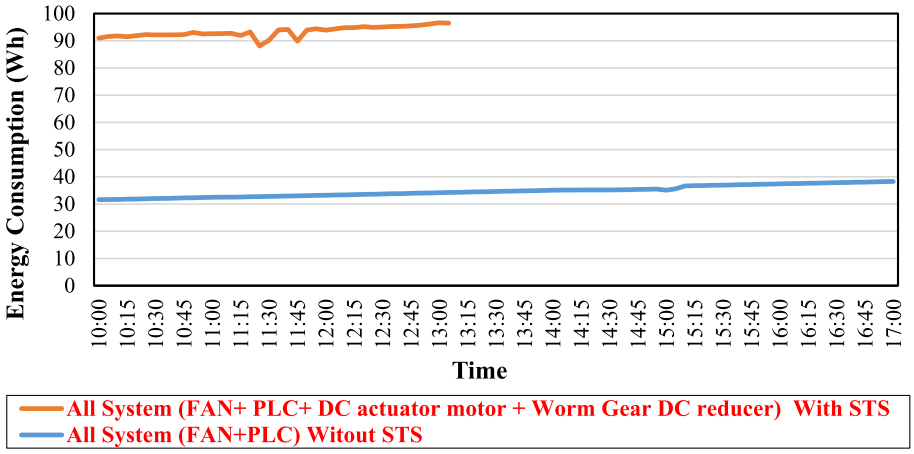

Fig. 9. Energy consumption values for the all system.

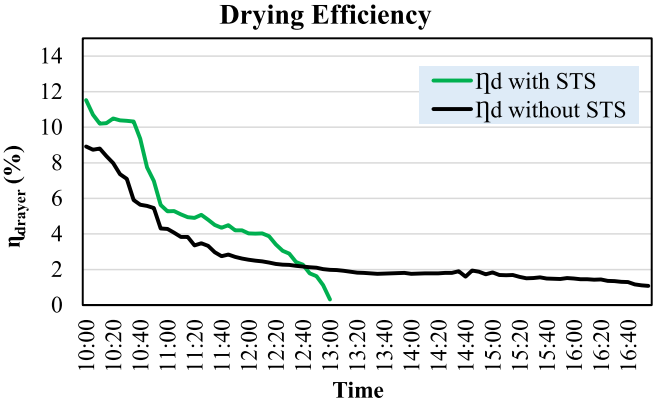

Fig. 10. Variation of drying efficiency of the system without and with STS over time.

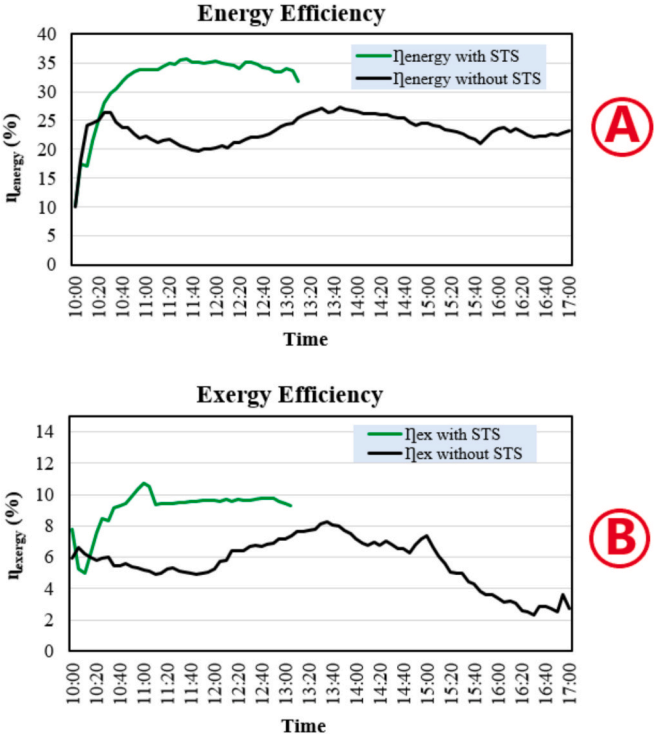

Fig. 11. Variation of energy (A) and exergy (B) efficiencies of PTSC vs. STS over time.

calculated payback period of 0.76 years indicates that the system is also economically competitive.

In summary, compared to current solar-assisted drying systems in the literature, the proposed system demonstrates high energy, exergy, and drying efficiency due to its PTSC integration, dual-axis solar tracking system, and natural flow structure. The observed trends—high surface temperature, short drying time, and increased energy efficiency—are consistent with the existing literature, clearly highlighting the innovative aspects of the system.

4. Conclusions

This study experimentally evaluated the performance of a greenhouse-type drying system equipped with a dual-axis STS integrated into a PTSC. The STS-supported system demonstrated significant performance improvements compared to a conventional without STS drying system operating under the same conditions.

According to the experimental results, the drying time was reduced by 55 % in the STS-equipped system, optimizing both process time and energy consumption. Energy efficiency was measured at 31.8 %, and exergy efficiency at 9.18 %; these values were 23.2 % and 5.74 %, respectively, in the STS-less system. Additionally, the product surface temperature reached an average of 77.4 °C with STS, remaining at 47.3 °C in the system without STS. With the help of STS, the system operated under an average solar radiation of 784.3 W/m^2 and created an efficient drying environment through natural radiation and directed heat transfer provided via the PTSC. A significant increase in drying efficiency was observed in the STS system compared to the system without STS.

Table 8
Comparison of System Performance Parameters With and Without Dual-Axis Solar Tracking System.

Parameter	With STS	Without STS
Energy Efficiency	31.8 %	23.2 %
Exergy Efficiency	9.2 %	5.7 %
Tube Outlet Temperature	80 °C	57.2 °C
Drying Efficiency	9.5 %	5 %
Measured Solar Radiation (*SR*)	784 W/m^2	664 W/m^2

The present study provides a reference point for designing PTSC systems and applications to improve energy efficiency while contributing to sustainable energy technologies. In addition, this study provides a solid foundation for researchers working on solar drying systems to

develop low-cost, environmentally friendly, and high-performance solutions. Scientifically, it significantly contributes to the academic literature and practical engineering applications by providing a new perspective at the intersection of energy conversion, thermodynamic optimization, and food drying technologies. Plans include testing the system in larger-scale applications, performing optimizations for drying different agricultural products, and integrating fully automated AI-based control systems.

CRediT authorship contribution statement

Mehmet Das: Writing – review & editing, Writing – original draft, Software, Methodology, Formal analysis, Conceptualization. **Oguzhan Pektezel:** Writing – review & editing, Resources, Formal analysis, Data curation. **Mithat Sımsek:** Writing – review & editing, Project administration, Data curation.

Declaration of Competing Interest

The authors declare that they have no known competing financial interests or personal relationships that could have appeared to influence the work reported in this paper.

Acknowledgments

This study was supported by the Tokat Gaziosmanpaşa University (TOGU) - Scientific Research Projects Coordination Unit under Grant Number 2022/46. The authors thank TOGU for their support.

References

[1] S.A. Mousavi Rabeti, M.H. Khoshgoftar Manesh, M. Amidpour, Techno-economic and environmental assessment of a novel polygeneration system based on integration of biomass air-steam gasification and solar parabolic trough collector, Sustain. Energy Technol. Assessments 56 (2023) 103030, https://doi.org/10.1016/j.seta.2023.103030.

[2] M. Öztürk, C. Yüksel, E. Çiftçi, Energy, exergy and sustainability analysis of a photovoltaic-thermal solar system with nano-enhancement and thermal energy storage integration, Process Saf. Environ. Prot. 187 (2024) 593–604, https://doi.org/10.1016/j.psep.2024.05.026.

[3] S.K. Sahu, A.S. Kopalakrishnaswami, S.K. Natarajan, Historical overview of power generation in solar parabolic dish collector system, Environ. Sci. Pollut. Res. 29 (2022) 64404–64446, https://doi.org/10.1007/s11356-022-21984-3.

[4] A. Keçebaş, O.V. Güler, A.G. Georgiev, E.Y. Gürbüz, A.D. Tuncer, İ. Şahinkesen, Thermodynamic analysis and efficiency enhancement of PV/T systems using ethanol-based phase change material, Energy 320 (2025), https://doi.org/10.1016/j.energy.2025.135165.

[5] A. Nešović, N. Lukić, R. Kowalik, A. Janaszek, D. Taranović, T. Kozłowski, Experimental and numerical comparison of glass tube collector with relative single-axis tracking and flat-plate collector without tracking during cloudy-sky days, Sol. Energy 291 (2025), https://doi.org/10.1016/j.solener.2025.113412.

[6] Z. Zhao, F. Bai, X. Zhang, Z. Wang, Experimental study of pin finned receiver tubes for a parabolic trough solar air collector, Sol. Energy 207 (2020) 91–102, https://doi.org/10.1016/j.solener.2020.06.070.

[7] M.O. Karaağaç, B. Akıncı, A. Ergün, Enhancing the performance of parabolic trough solar collectors: cost-effective innovative designs for sustainable energy harvesting, Appl. Therm. Eng. 253 (2024), https://doi.org/10.1016/j.applthermaleng.2024.123693.

[8] F. Ben Othman, F. Eddhibi, A. Bel Hadj Ali, A. Fadhel, Ö. Bayer, İ. Tarı, A. Guizani, M. Balghouthi, Investigation of olive mill sludge treatment using a parabolic trough solar collector, Sol. Energy 232 (2022) 344–361, https://doi.org/10.1016/j.solener.2022.01.008.

[9] S. Nain, V. Ahlawat, S. Kajal, P. Anuradha, A. Sharma, T. Singh, Performance analysis of different U-shaped heat exchangers in parabolic trough solar collector for air heating applications, Case Stud. Therm. Eng. 25 (2021) 100949, https://doi.org/10.1016/j.csite.2021.100949.

[10] A.A. Mathew, V. Thangavel, N.A. Mandhare, M.R. Nukulwar, Latent and sensible heat thermal storage in a heat pipe-based evacuated tube solar dryer: a comparative performance analysis, J. Energy Storage 57 (2023) 106305, https://doi.org/10.1016/j.est.2022.106305.

[11] Y. Guan, L. Zhou, W. Hu, Z. Wei, G. Li, Y. Liu, K. Ma, Comparative analysis of the thermal performances of two parabolic trough solar air collectors used for greenhouse heating: an experimental study, Therm. Sci. Eng. Prog. 62 (2025), https://doi.org/10.1016/j.tsep.2025.103666.

[12] T. Limboonruang, M. Oyinlola, D. Harmanto, N. Phunapai, Optimizing the configuration of external fins of solar receiver tubes for the solar parabolic trough collector, Appl. Therm. Eng. 263 (2025) 125317, https://doi.org/10.1016/j.applthermaleng.2024.125317.

[13] H. Parlamış, E. Özden, M.S. Büker, Experimental performance analysis of a parabolic trough solar air collector with helical-screw tape insert: a comparative study, Sustain. Energy Technol. Assessments 47 (2021), https://doi.org/10.1016/j.seta.2021.101562.

[14] P. Singh, B.K. Pandey, M.K. Gaur, Performance evaluation of evacuated solar collector assisted hybrid greenhouse solar dryer under active and passive mode, Mater. Today Proc. (2021), https://doi.org/10.1016/j.matpr.2021.10.461.

[15] B. Stanek, D. Węcel, Ł. Bartela, S. Rulik, Solar tracker error impact on linear absorbers efficiency in parabolic trough collector – Optical and thermodynamic study, Renew. Energy 196 (2022) 598–609, https://doi.org/10.1016/j.renene.2022.07.021.

[16] M. Gharzi, A.M. Kermani, H. Tash Shamsabadi, Experimental investigation of a parabolic trough collector-thermoelectric generator (PTC-TEG) hybrid solar system with a pressurized heat transfer fluid, Renew. Energy 202 (2023) 270–279, https://doi.org/10.1016/j.renene.2022.11.110.

[17] B. Wang, Q. Xu, Y. Yang, Design and implementation of a novel automated sun tracking system for distributed heating using parabolic trough solar collector, Appl. Therm. Eng. 274 (2025), https://doi.org/10.1016/j.applthermaleng.2025.126607.

[18] H. Fathabadi, Novel low-cost parabolic trough solar collector with TPCT heat pipe and solar tracker: Performance and comparing with commercial flat-plate and evacuated tube solar collectors, Sol. Energy 195 (2020) 210–222, https://doi.org/10.1016/j.solener.2019.11.057.

[19] T.Q. Saldivar-Aguilera, L.M. Valentín-Coronado, M.I. Peña-Cruz, A. Diaz-Ponce, J. A. Dena-Aguilar, Novel closed-loop dual control algorithm for solar trackers of parabolic trough collector systems, Sol. Energy 259 (2023) 381–390, https://doi.org/10.1016/j.solener.2023.05.024.

[20] N. Arbaoui, R. Tadili, M. El Baz, I. Ihoume, H. Essalhi, M. Daoudi, N. Wahid, J. Aabdousse, Impact of a solar greenhouse converted into a solar dryer on the performance indicators (energy efficiency, bio-chemical, economic and environmental) during summer season, Sol. Energy 291 (2025) 113416, https://doi.org/10.1016/j.solener.2025.113416.

[21] E.E. Tiguh, M.A. Delel, A.N. Ali, G.K.M. Gelaw, S.W. Fanta, M. Bayable, Development and performance evaluation of greenhouse solar dryer for unthreshed Teff crops, Results Eng. 25 (2025) 104495, https://doi.org/10.1016/j.rineng.2025.104495.

[22] A. Zine A. Benseddik R. Saim M. Zelaci A. Laouini K. Mansouri M.A. Kherrafi M.T. Oucif Khaled S. Guediri Performance and sustainability assessment of a greenhouse dryer with integrated sunlight protection for mint drying, Renew. Energy 244 2025 10.1016/j.renene.2025.122723.

[23] S. Rajesh, S. Sekar, S.D. Sekar, S. Madhankumar, Drying kinetics, energy, statistical, economic, and proximate analysis of a greenhouse dryer using different glazing materials for Coccinia grandis drying, Sol. Energy 284 (2024) 113047, https://doi.org/10.1016/j.solener.2024.113047.

[24] P.M. Patel, V.P. Rathod, V.K. Patel, Development and enhancement in drying performance of a novel portable greenhouse solar dryer, J. Stored Prod. Res. 105 (2024) 102228, https://doi.org/10.1016/j.jspr.2023.102228.

[25] R. Sehrawat, R.K. Sahdev, D. Chhabra, S. Tiwari, Experimentation and optimization of phase change material integrated passive bifacial photovoltaic thermal greenhouse dryer, Sol. Energy 257 (2023) 45–57, https://doi.org/10.1016/j.solener.2023.04.024.

[26] N. Philip, S. Duraipandi, A. Sreekumar, Techno-economic analysis of greenhouse solar dryer for drying agricultural produce, Renew. Energy 199 (2022) 613–627, https://doi.org/10.1016/j.renene.2022.08.148.

[27] C.S. Koli, M.K. Gaur, P. Singh, Energy and exergy assessment of a novel parabolic hybrid active greenhouse solar dryer, Sol. Energy 245 (2022) 211–223, https://doi.org/10.1016/j.solener.2022.09.021.

[28] F. Selimefendigil, C. Şirin, K. Ghachem, L. Kolsi, Exergy and environmental analysis of an active greenhouse dryer with Al2O3 nano-embedded latent heat thermal storage system: an experimental study, Appl. Therm. Eng. 217 (2022), https://doi.org/10.1016/j.applthermaleng.2022.119167.

[29] S. Singh, R.S. Gill, V.S. Hans, T.C. Mittal, Experimental performance and economic viability of evacuated tube solar collector assisted greenhouse dryer for sustainable development, Energy 241 (2022) 122794, https://doi.org/10.1016/j.energy.2021.122794.

[30] P. Singh, M.K. Gaur, Environmental and economic analysis of novel hybrid active greenhouse solar dryer with evacuated tube solar collector, Sustain. Energy Technol. Assessments 47 (2021) 101428, https://doi.org/10.1016/j.seta.2021.101428.

[31] P. Singh, M.K. Gaur, Heat transfer analysis of hybrid active greenhouse solar dryer attached with evacuated tube solar collector, Sol. Energy 224 (2021) 1178–1192, https://doi.org/10.1016/j.solener.2021.06.050.

[32] R. Karthikeyan, P. Thangavel, R.T. Raghunath, K.A. Muthu Priyan, M. Praveen Balaji, Performance analysis of greenhouse solar dryer using evacuated tubes, Mater. Today Proc. 66 (2022) 1509–1513, https://doi.org/10.1016/j.matpr.2022.06.447.

[33] G. Çakmak, C. Yildiz, The prediction of seedy grape drying rate using a neural network method, Comput. Electron. Agric. 75 (2011) 132–138, https://doi.org/10.1016/j.compag.2010.10.008.

[34] P. Russo, G. Adiletta, M. Di Matteo, The influence of drying air temperature on the physical properties of dried and rehydrated eggplant, Food Bioprod. Process. 91 (2013) 249–256, https://doi.org/10.1016/j.fbp.2012.10.005.

[35] S. Kalogirou, Parabolic Trough Collector System for Low Temperature Steam Generation: Design and Performance Characteristics, Appl. Energy 55 (1996) 1–19, https://doi.org/10.1016/S0306-2619(96)00008-6.

[36] B.K. Bala Drying and Storage of cereal grains 2017 Wiley Blackwell.
[37] C. Kumar, M.A. Karim, M.U.H. Joardder, Intermittent drying of food products: a critical review, J. Food Eng. 121 (2014) 48–57, https://doi.org/10.1016/j.jfoodeng.2013.08.014.
[38] M. Das, E.K. Akpinar, Investigation of the effects of solar tracking system on performance of the solar air dryer, Renew. Energy 167 (2021) 907–916, https://doi.org/10.1016/j.renene.2020.12.010.
[39] M. Das, E. Alic, E.K. Akpinar, Detailed analysis of mass transfer in solar food dryer with different methods, Int. Commun. Heat Mass Transf. 128 (2021) 105600, https://doi.org/10.1016/j.icheatmasstransfer.2021.105600.
[40] S.E. Bousbia Salah, A. Benseddik, N. Meneceur, A. Zine, K. Deghoum, Design and realization of a new solar dryer assisted by a parabolic trough concentrator (PTC) with a dual-axis solar tracker, Sol. Energy 283 (2024) 113001, https://doi.org/10.1016/j.solener.2024.113001.
[41] E.Z. Moya, Parabolic-trough concentrating solar power (CSP) systems, Conc. Sol. Power Technol. (2012) 197–239, https://doi.org/10.1533/9780857096173.2.197.
[42] W. Wang, M. Li, R.H.E. Hassanien, Y. Wang, L. Yang, Thermal performance of indirect forced convection solar dryer and kinetics analysis of mango, Appl. Therm. Eng. 134 (2018) 310–321, https://doi.org/10.1016/j.applthermaleng.2018.01.115.
[43] H. Samimi Akhijahani, P. Salami, M. Iranmanesh, M.S.B. Jahromi, Experimental study on the solar drying of Rhubarb (Rheum ribes L.) with parabolic trough collector assisted with air recycling system, nanofluid and energy storage system, J Energy Storage 60 (2023) 106451, https://doi.org/10.1016/j.est.2022.106451.
[44] R. Petela, Exergy of heat radiation, J. Heat Transfer 86 (1964) 187–192, https://doi.org/10.1115/1.3687092.
[45] M. Libra, D. Mrázek, I. Tyukhov, L. Severová, V. Poulek, J. Mach, T. Šubrt, V. Beránek, R. Svoboda, J. Sedláček, Reduced real lifetime of PV panels – Economic consequences, Sol. Energy 259 (2023) 229–234, https://doi.org/10.1016/j.solener.2023.04.063.
[46] S. Abdelhady, Performance and cost evaluation of solar dish power plant: sensitivity analysis of levelized cost of electricity (LCOE) and net present value (NPV), Renew. Energy 168 (2021) 332–342, https://doi.org/10.1016/j.renene.2020.12.074.
[47] H. Fathabadi, Impact of utilizing reflector, single-axis and two-axis sun trackers on the performance of an evacuated tube solar collector, Int. J. Green Energy 17 (2020) 742–755, https://doi.org/10.1080/15435075.2020.1798766.
[48] M.S. Büker, H.I. Parlamis, M. Alwetaishi, O. Benjeddou, Experimental investigation on the dehumidification performance of a parabolic trough solar air collector assisted rotary desiccant system, Case Stud. Therm. Eng. 34 (2022), https://doi.org/10.1016/j.csite.2022.102077.
[49] N.I. Tsongidis, C.A. Poravou, C. Lekkos, G. Karagiannakis, B. Ulkutasir, D. Baker, Hydrothermal liquefaction of agri-food waste : Concentrated solar thermal coupling with a sensible heat storage system, in: In: 11th International Conference on Sustainable Solid Waste Management, 2024, pp. 12–13.
[50] S. Naaim, B. Ouhammou, M. Aggour, B. Daouchi, E.M. El Mers, M. Mihi, Multi-Utility Solar thermal Systems: Harnessing Parabolic Trough Concentrator using SAM Software for Diverse Industrial and Residential applications, Energies 17 (2024), https://doi.org/10.3390/en17153685.
[51] S. Audrey Heugang Ndjanda, E. Tchoffo Houdji, Heat transfer fluids and external convection effects on transient thermodynamic behavior of a parabolic trough solar collector in Sahelian climate, Exergy - Theor. Backgr. Cases Study [working Title] (2024) 1–29, https://doi.org/10.5772/intechopen.1004596.
[52] S. Bori, I. Jiya, J.Y. Orah, A.M. Bako, Heat transfer Analysis of a Concentrated-Type Solar Dryer for Ginger, Gazi Univ. J. Sci. 11 (2024) 690–700. https://doi.org/10.54287/gujsa.1538840.
[53] S. Liu, B. Yang, X. Yu, Thermal transfer characteristics and thermoelasticity analysis of direct-steam-generation parabolic trough collector, Renew. Energy 234 (2024) 121264, https://doi.org/10.1016/j.renene.2024.121264.
[54] M. Halimi, I. Outana, A. El Amrani, J. Diouri, C. Messaoudi, Prediction of captured solar energy for different orientations and tracking modes of a PTC system: Technical feasibility study (Case study: South eastern of MOROCCO), Energy Convers. Manag. 167 (2018) 21–36, https://doi.org/10.1016/j.enconman.2018.04.051.
[55] S.E. Bousbia Salah, A. Benseddik, N. Meneceur, A. Zine, K. Deghoum, Design and realization of a new solar dryer assisted by a parabolic trough concentrator (PTC) with a dual-axis solar tracker, Sol. Energy 283 (2024), https://doi.org/10.1016/j.solener.2024.113001.
[56] A.A. Elsayed, E.E. Khalil, M.A. Kassem, O.A. Huzzayin, A novel mechanical solar tracking mechanism with single axis of tracking for developing countries, Renew. Energy 170 (2021) 1129–1142, https://doi.org/10.1016/j.renene.2021.02.058.
[57] M. Kumar, P.V. Prabhansu Bhale, Experimental investigation on dual-shaped solar greenhouse dryer: Performance and technoeconomic analysis, J. Stored Prod. Res. 112 (2025) 102621, https://doi.org/10.1016/j.jspr.2025.102621.